Mechanical Characterization of Polymers on a Nanometer Scale through Nanoindentation. A Study on Pile-up and Viscoelasticity

Davide Tranchida,[†] Stefano Piccarolo,[*,†] Joachim Loos,[‡,§] and Alexander Alexeev[‡,||]

Dipartimento di Ingegneria Chimica dei Processi e dei Materiali, Viale delle Scienze, University of Palermo, Palermo, Italy, Department of Chemical Engineering and Chemistry, Eindhoven University of Technology, P.O. Box 513, 5600 MB Eindhoven, The Netherlands, Dutch Polymer Institute, P. O. Box 902, 5600 AX Eindhoven, The Netherlands, and NT-MDT, 124460 Moscow, Russian Federation

Received September 15, 2006

ABSTRACT: The analysis of nanoindentation force curves collected on polymers through the common Oliver and Pharr procedure does not lead to a correct evaluation of Young's modulus. In particular, the estimated elastic modulus is several times larger than the correct one, thus compromising the possibility of a nanomechanical characterization of polymers. Pile-up or viscoelasticity is usually blamed for this failure, and a deep analysis of their influences is attempted in this work. Piling-up can be minimized by indenting on a true nanometer scale, i.e., at penetration depth smaller than 200 nm. On the other side, it is common knowledge that fast indentations minimize the effect of viscoelasticity. However, changing the indentation time in a broad range of contact time (fractions of second up to hundreds of seconds) did not allow the correct estimation of Young's modulus for the polymers used in this work. The final result is that the Oliver and Pharr procedure as well as any other procedure analyzing the unloading curve with elastic contact mechanics models cannot be employed to measure Young's modulus of polymers because its application is incorrect from a theoretical point of view, unless the analysis is limited to the very first nanometers of penetration depth when the contact is perfectly elastic. Viscoelastic contact mechanics models should instead be employed to characterize these materials.

Introduction

The mechanical characterization of polymers on nanometer scale might be a useful tool in polymer science for several reasons. For example, mapping local mechanical properties is possible on samples characterized by variation of composition as well as heterogeneity induced by solidification during processing or complex morphology as arising in biological samples. Nanoindentation is a powerful tool to this purpose, but the technique currently shows some challenges. It is indeed quite well-known that the same procedures used to characterize the mechanical properties of metals or ceramics do not allow the correct measurement of polymers' mechanical properties.[1] The reasons for this failure are usually found in the pile-up, which changes the contact area with respect to the one calibrated on standard material, or in the viscoelastic nature of polymers, which influences the unloading curve and does not even allow in many circumstances its fitting according to the common procedures.[2] For this latter reason, for example, researchers usually try to perform nanoindentations at high rates.[3]

In general, the unloading part of a force curve, i.e., a plot of applied load, F, vs penetration depth, p, is supposed to show merely the elastic behavior of the material. Sneddon[4] suggested a solution for the penetration of rigid bodies, characterized by simple geometries, into an elastic half-space in the limit of classical elasticity theory, i.e., reversible deformations. Oliver and Pharr[2] used the relations from Sneddon to develop a procedure to estimate Young's modulus of the sample from the slope of the unloading portion of a force curve obtained indenting a material with a conical indenter basing this assumption on the concept that initial unloading should be dominated by the elastic recovery. This procedure consists of a double calibration to estimate the machine compliance and the area function, i.e., the contact area from the contact depth. Since their first paper, several corrections were suggested to take into account radial displacements of the sample,[5] correction for true geometry[6] and either pile-up or sinking-in of the original surface.[7] Corrections to the Oliver and Pharr (O&P) procedure for a spherical indenter were also introduced by Field and Swain.[8]

Despite the wide use in the nanoindentation community, Loubet[9] and Hochstetter et al.[3] clearly pointed out that the Oliver and Pharr procedure is not applicable to polymers, due, for common conditions, to their peculiar viscoelastic mechanical behavior. The most remarkable phenomenon caused by viscoelasticity, appearing when performing nanoindentations at low loading rate or with short holding time, is a "nose"[10] in the force curve, with the penetration depth eventually increasing even during the unloading portion of the force curve. This phenomenon clearly implies that the O&P procedure, fitting the unloading curve with a power law relation, cannot be applied, yielding unreasonably high or even negative slopes as predicted by the theoretical analysis of Ting.[11] However, even if viscoelastic effects are minimized, another point well-known to practitioners is the inaccuracy in the elastic modulus measurement through the O&P procedure when performing the area function calibration on fused silica, as recommended. A common procedure for polymers is then to calibrate the area function on polycarbonate rather than fused silica (see, e.g., Hengsberger et al.[12]). Doubts arise about the reliability of the calibration on arbitrary materials since Troyon and Huang[13] showed that the calibrated area function changes when using fused quartz or titanium as a standard sample, or also in connection to the work of Ikezawa and Maruyama,[14] who showed that there was a

* Corresponding author. E-mail: Piccarolo@unipa.it.
† Dipartimento di Ingegneria Chimica dei Processi e dei Materiali, Viale delle Scienze, University of Palermo.
‡ Department of Chemical Engineering and Chemistry, Eindhoven University of Technology.
§ Dutch Polymer Institute.
|| NT-MDT.

10.1021/ma062140k CCC: $37.00
Published on Web 01/20/2007

significant discrepancy between the measured geometry and the one inferred from the instrumented indentation data. This argument is even more dramatic in the case of polymeric samples for which the calibration of the area function is not traceable. A further criticism to the O&P approach is provided by a recent contribution by Chaudri[15] and Lim and Chaudri,[16] who pointed out that the use of the so-called reduced modulus, which takes into account the elastic properties of both the indenter and the material, is incorrect to account for displacement in the indenter. The indenter, whether diamond or silicon, is a much stiffer material than the sample in the case of polymer indentation, and it can be modeled as a rigid body without introducing any error.

Another difficulty for polymers' nanoindentation arises from the complex mechanical behavior related to different morphologies.[17] Indeed, mechanical properties do not depend only on the chemical composition nor on the primary structure of the backbone chain (molecular weight, tacticity, branching, and so forth).[18] Morphology, i.e., the microstructure developed during sample preparation,[19] always plays a dramatic role and there are several examples of polymers noticeably changing properties and morphology, for example, depending on the cooling rate from the melt[20] or on pressure.[21] Processing, i.e., shaping from the melt, always involves heterogeneous solidification conditions giving rise to an heterogeneous morphology. For this reason, a comparison between Young's modulus from macroscopic tests (which homogenize the mechanical behavior of the whole sample) and the one calculated from instrumented indentation tests (which in turn is a very local measurement) can be possible only if the polymeric sample is homogeneous and if such local properties are representative for the whole. This is not a trivial requirement, but is often unaddressed in the literature, while vice versa particular care is taken in this work by adopting a procedure recently developed[20] to solidify polymer films of a sufficient extension such as to make a macroscopic mechanical characterization as well as, obviously, one on the nanometer scale.

Experimental Section

The nanoindentation system used in this study was an assembly of a NT−MDT atomic force microscope (AFM) with the standard head replaced by a Triboscope indentor system (Hysitron Inc., Minneapolis, MN). The Hysitron system allows one to apply a certain load on the indenter by means of an electrostatic force acting on the transducer.

Instrument compliance was calibrated on fused silica. A Berkovich indenter, with equivalent semi-opening angle of 70.3°, was used with the area function calibrated on fused silica according to O&P as also described in the results part. Indentations were performed in load-controlled and displacement-controlled mode after collecting images of the area to be indented, in order to check surface roughness in the selected area. In both displacement and load controlled mode, either penetration or load is initially ramped at constant rate up to the selected value, kept constant for 10 s and brought back to zero. The applied load varies between 10 and 140 μN in the case of polymers and between 50 and 7000 μN for fused silica while loading rate ranges between 1 and 100 μN/s. For displacement controlled experiments penetration depth changes in the range 20−300 nm with a penetration rate in the range 1−300 nm/s. Thermal drift was measured and corrected for each indentation. Further analysis was performed at larger loads with the MicroMaterials Nanotest600 at MicroMaterials Ltd., Wrexham, U.K.

The polymers used in this work were glassy amorphous and semicrystalline ones, atactic polystyrene, PS N5000 from Nova Chemicals, polycarbonate, PC Lexan 121R from GE Plastics, and isotactic polypropylene, iPP, respectively, trade name T30G, kindly supplied by Montell. For iPP, the samples were prepared under different solidification conditions from the melt[22] spanning cooling rates typical of processing,[20] thus developing quite different morphologies of the same material. Once the sample reaches the final temperature it is immediately removed from the sample assembly and kept at low temperature (−30 °C) before further characterization in order to prevent structure evolution. Depending on the morphology, such samples have different mechanical properties; for example, Young's modulus varies between 1.2 GPa for the semicrystalline one (cooling rate 2.5 K/s) and 700 MPa (888 K/s) for an iPP sample where the typical mesomorphic morphology was developed throughout the whole sample, i.e., homogeneously.[17] Mesomorphic samples, although metastable, once aged at room temperature for a few hours do not show changes of Young's modulus.[23]

Results

On such a broad range of polymers and polymer morphologies (glassy amorphous, mesomorphic and semicrystalline below and above glass transition temperature) nanoindentation experiments are next discussed determining the elastic modulus by the common O&P procedure highlighting its deviations with respect to bulk modulus. Since it is commonly assumed that sources of deviations depend on pile-up, which determines a change of the area function with respect to the calibrating material, and viscoelasticity, which causes the onset of a "nose" in the unloading portion of the force curve, the influence of these two factors are discussed in some detail. The choice of experimental conditions that, according to Oliver and Pharr,[24] minimize the extent of pile-up does not improve the modulus evaluation with their procedure. At the same time, high loading rates, that prevent the development of the "nose" , do not affect considerably the modulus evaluation thus questioning the common knowledge about the failure of the O&P procedure when applied to polymers. A discussion about the correct reasons for this failure will be also provided, together with recommendations for further studies.

Young's Modulus of Some Selected Polymers. Following the procedure introduced by O&P, the machine compliance and the area function were first calibrated. Because of the compliance of the polymeric samples, considerable penetration depths were obtained already at tiny loads, so that the machine compliance correction is almost negligible. Its calibration was, however, performed in order to comply with the O&P procedure. For this purpose, nanoindentations were carried out on fused silica at the maximum loads allowed by the Triboscope nanoindenter, in the range 0.05−7 mN for the area function calibration, since penetrations are the largest possible with this material and therefore closer to those obtained on polymers. It is worth noticing that the estimated hardness at this load level is found to be constant regardless of penetration depth and thus the O&P procedure can be used to estimate the load frame compliance that in this case amounts to 0.4 nm/mN. This one was afterward removed automatically so as to measure the net contact stiffness.

The area function, i.e., the relation between contact depth and contact area, was calibrated performing several indentations on fused silica with penetration depths in the range 10−220 nm, Figure 1, with good reproducibility. The power law fitting of the unloading curves resulted in an exponent, n, close to 1.35, as shown in the inset of Figure 1 and in agreement with the value reported in the literature.[24] It can be noted that the unloading exponent value at low loads is larger than the one obtained at high loads. This occurrence can be explained as the effect of the inevitable tip rounding at the apex, conjecture also confirmed once one notices that an exponent close to 1.5 is

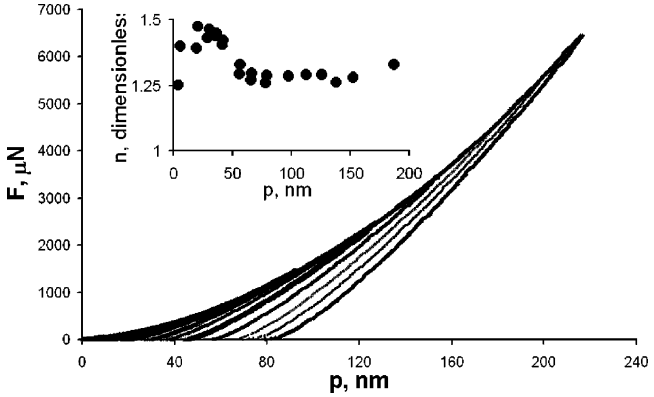

Figure 1. Force curves for the standard fused silica sample, used for area function calibration, covering the range of penetration depth used for polymer nanoindentations of this work. Inset shows the unloading exponent, *n* in eq 1, in agreement with common knowledge.

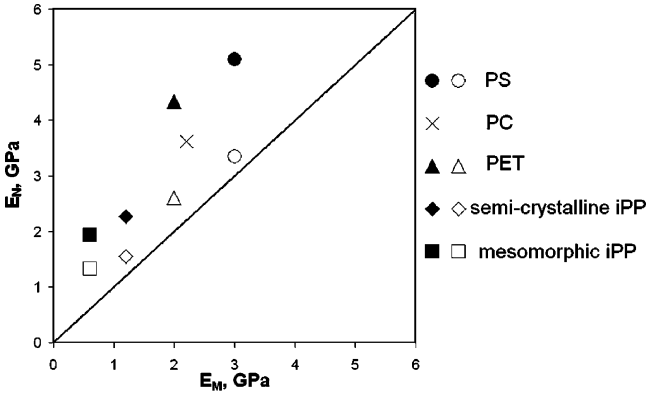

Figure 2. Elastic moduli evaluated by Oliver and Pharr procedure from force curves obtained by nanoindentation, E_N, vs macroscopic moduli, E_M, for a broad range of polymer samples and polymer morphologies. Moduli obtained from nanoindentations were obtained with both area function calibration from fused silica (see Figure 1), filled symbols, and area function from PC, open symbols.

indeed predicted by elastic contact models for sphere or paraboloid indenter geometries. The reduced elastic modulus of fused silica (E_r = 69.6 GPa) was used as an input in order to evaluate the contact area at each contact depth, and the plot was fitted with the dependence prescribed by O&P obtaining the area function.

Force curves were collected in order to measure Young's modulus of several polymers within a broad range of experimental conditions, i.e., different material elastic moduli, penetration rates, loading rates, penetration depth, and applied load. Values of contact stiffness S and contact depth h_c, and therefore of contact area A_c, were evaluated from each force curve. The elastic modulus can then be evaluated by the O&P procedure using three parameters (usually called β, ϵ, γ), although the choice of their values is not straightforward and often source of errors.

The first one, ϵ, is a geometrical parameter[25] whose value is often taken equal to 0.75 for a Berkovich indenter. Recently Martin and Troyon[26] showed that this value has to be evaluated for each force curve from the unloading exponent n. Even though it changes slightly in the normal operating conditions of metals or ceramics,[26] where n is bounded between 1 and 2, its value is definitely more debatable for polymers as it will be shown in the following.

The correction factor β is a purely geometrical factor[6] taking into account that the indenter is not a perfect cone although it does not account for the finite radius of curvature of the indenter. King[6] determined by FEM simulations for the Berkovich indenter a value of β of 1.034.

The correction factor γ arises from the improper account in Sneddon's solution for radial material displacement into the contact region.[5] Following Hay et al.,[5] the value of this correction parameter, dependent on sample Poisson ratio and the indenter half included angle, takes, for a Berkovich indenter and typical Poisson ratio of 0.3, the value 1.067.

The O&P analysis was performed with these correction factors and the values for contact stiffness and contact depth from the force curves collected on all the materials studied in this work. The Young's moduli obtained from nanoindentations, E_N, performed in load controlled mode with a loading rate of 30 μN/s are plotted in Figure 2 as the filled series against the true elastic moduli measured through macroscopic tests, E_M.

As can clearly be seen, the disagreement is severe, overestimating Young's modulus by 1.7−3.2 times as shown in Table 1 for the standard calibration of area function on fused silica. It is worth mentioning that the magnitude of this deviation is so large that it cannot be due to a wrong choice of the abovementioned correction factors, which can change the results of up to ca. ±15%.

Table 1. Deviations of the Nanoindentation Determined Young's Modulus, E_N, with Respect to the One Measured by Macroscopic Tests, E_M

sample	E_N/E_M
PS	1.70
PC	1.64
PET	2.17
semicrystalline iPP	2.10
mesomorphic iPP	3.22

The unusual high values found for the elastic moduli could be explained with the observation that a compression modulus is being measured through nanoindentations, and it can be larger than the one macroscopically measured through tensile tests. However, the magnitude of the deviation makes this conjecture quite unreasonable when considering that for most polymers compressive and tensile elastic moduli differ at most of 20%.

A solution sometimes adopted in the literature is to calibrate the area function on another polymer, showing both viscoelastic and piling-up behavior.[12] A PC sample was chosen to estimate a new area function, through indentations performed in the range of penetration depth of 10−200 nm. The force curves were analyzed with the new area function, obtained by the same procedure used for fused silica but using as an input the reduced elastic modulus of PC measured from macroscopic tests, and the results are shown in Figure 2 as the empty series. Obviously, the agreement is perfect for PC because it was the calibrating material, but deviations are again consistently higher than the bulk Young's modulus as one moves the attention to softer materials.

Since the material, surrounding the zone where the stress field is concentrated, acts as a constraint, it is expected that Young's modulus measured by nanoindentations is larger than the bulk one measured by macroscopic tests. This effect would be obviously dramatic in the case of an incompressible material and full confinement, but even if the Poisson ratio is smaller than 0.5, an increase of elastic modulus is reasonable. However, the nanoindentation test does not take place in a fully confined geometry, and the material around the indentation can, to some extent, deform. Therefore, the confinement effect is expected to be smaller than in the case of full confinement and likely the increase in Young's modulus, although present, is considerably smaller than 35% as shown in the Appendix. In conclusion,

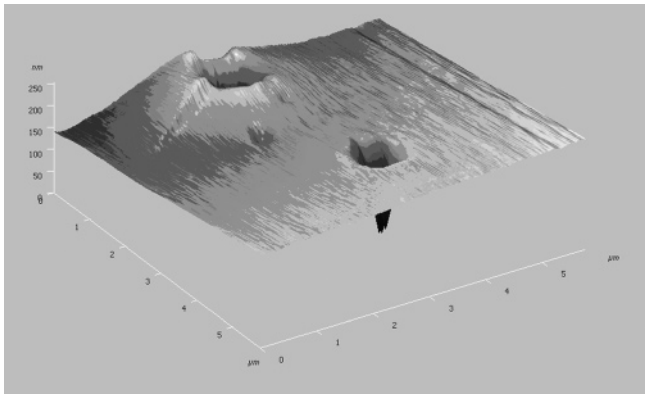

Figure 3. Topography of indentations showing the typical pile-up (bulging out of the surface on the left of the image) and a pile-up free nanoindentation (on the right).

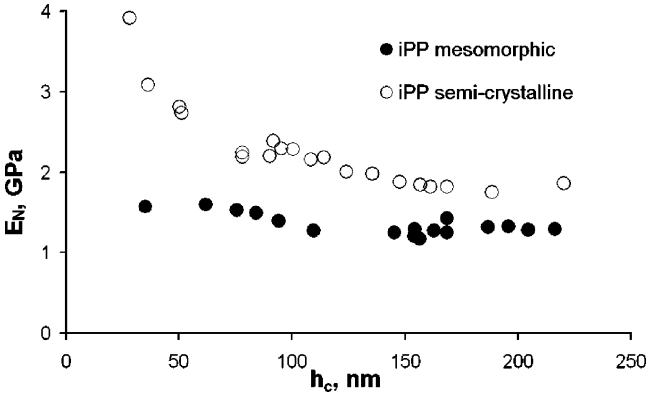

Figure 4. Dependence of elastic moduli, evaluated by the Oliver and Pharr procedure, on contact depth for two polymer samples with different properties (morphologies).

this contribution is not compatible nor can explain the unusual high values found in Figure 2 and table.1. *Besides that, it is not commonly observed when analyzing stiffer materials like metals or ceramics.*

In the following, we are discussing whether the reasons for such a failure could be identified in the piling-up and/or in the viscoelastic behavior of polymers.

Influence of Pile-up. The piling-up behavior is schematically shown in Figure 3 where two residual indentation imprints are shown. On the left, the piling-up, i.e., the bulging out of the free surface of the material during the indentation, is noticeable while, in the other imprint, it is not. Pile-up implies that the real contact area is larger than the one inferred from contact depth by the O&P procedure through calibration on a non piling-up material like fused silica. This occurrence thus implies that the material can accommodate a larger load and, as a result, the stiffness is apparently larger.

Although this argument could explain the abnormally large values of elastic moduli shown in Figure 2, the measurement should be correct at shallow penetration depths, when the material does not yet pile up.[7,24] A plot of estimated Young's modulus against penetration depth, shown in Figure 4 for the mesomorphic and semicrystalline iPP samples, can then provide some more insight. The onset of a well-known size scale effect[27] could explain the incorrect estimate at small penetration depth in Figure 4, where the elastic modulus is overestimated up to 4 times.

Following these results, one would conclude that size scale effects at small penetration depths and pile-up at large penetration depths imply that a nanomechanical characterization of

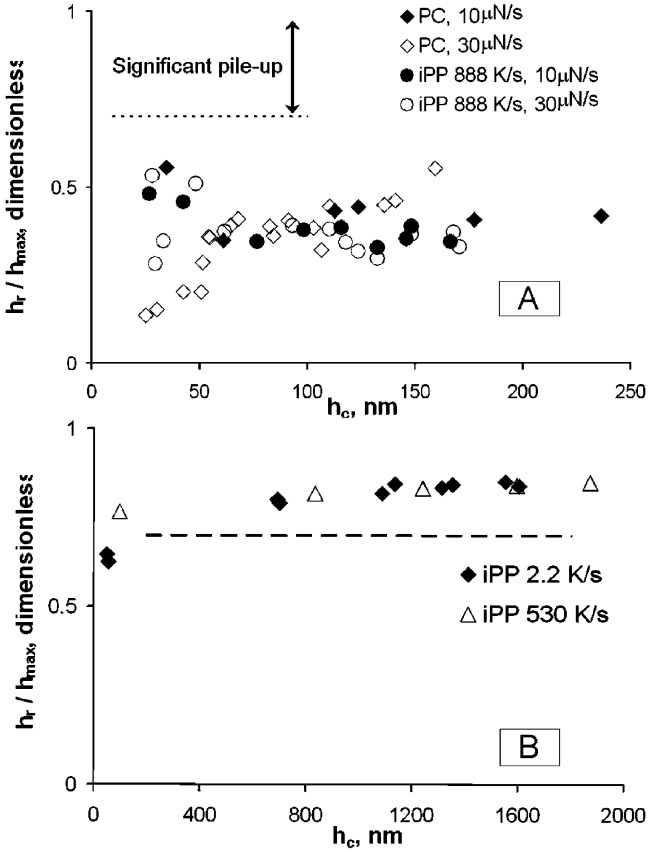

Figure 5. Effect of pile-up for (a) indentations at low and (b) for large penetration depths. The ratio on the ordinate is a measure of this effect; the threshold for onset of significant pile-up is also shown.[7,24]

polymers is not possible. The shape of the curve reported in Figure 4 is however quite surprising: at large penetration depths the estimated Young's modulus reaches a plateau while one would expect that the evaluated elastic modulus should increase as penetration depth increases, since pile-up should increase with penetration depth being related to the amount of plastic flow. The instrumental limitation on maximum penetration depth does not allow us to investigate whether the evaluated Young's modulus in Figure 4 converges toward the true macroscopic one at larger penetration depth. However, this discussion is of limited interest in the framework of this manuscript dealing with indentations on nanometer scale.

The importance of the phenomenon of pile-up is supposed to increase as the ratio E/σ_Y increases or with little capacity for work-hardening.[7,24] For the polymers studied in this work, the ratio E/σ_Y lies in the range 30−37. This value is not recognized in the literature[7,24] as responsible of large pile-up phenomena, because a threshold for the onset of pile-up effects has been suggested to take place when this ratio is above 90.[7,23] Concerning work-hardening, Oliver and Pharr[24] showed that, no matter what the work-hardening behavior of the material is, pile-up is not significant if the ratio of final indentation depth and maximum depth is below 0.7, a value which is expected to be constant regardless of penetration depth because of self-similarity of the Berkovich indenter. Figure 5a shows that this ratio is well below the threshold of 0.7 for two different materials studied: PC and a mesomorphic iPP tested at loading rates of 10 and 30 μN/s and at different load levels, resulting in penetration depths in the range 20−250 nm. This figure shows also that the ratio is nearly constant above ca. 50 nm while below this value, blunting of the indenter shape, causing a departure from the ideal cone geometry, affects the self-

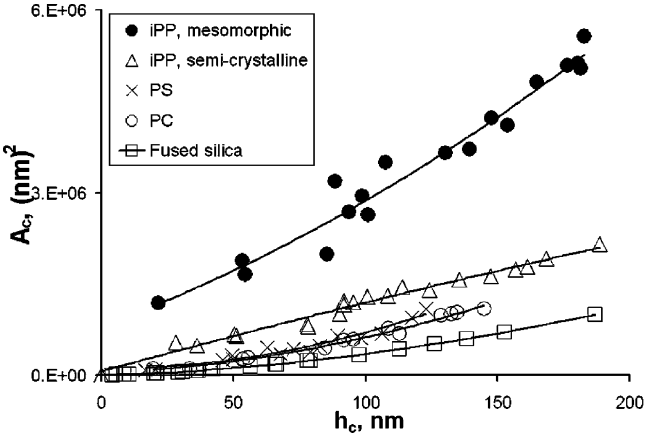

Figure 6. Apparent contact area function of all the samples tested in this work based on the macroscopic moduli used as an input.[2]

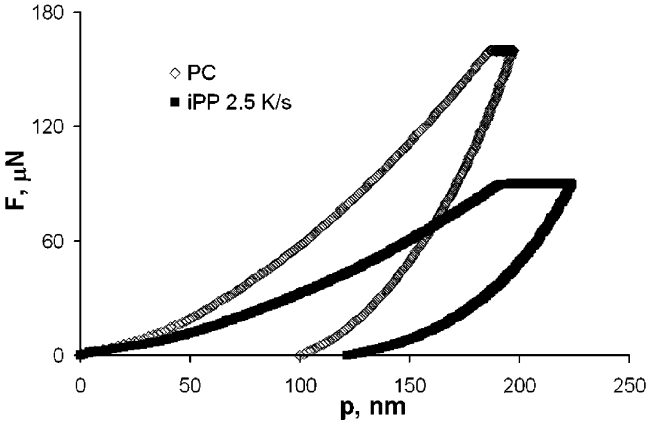

Figure 7. Force curves collected at high loading rates on PC and iPP so as to minimize viscoelastic effects. The "nose" caused by onset of viscoelastic effects (negative slope) is not observed.

similarity, and thus the ratio becomes quite scattered. Indentations were also performed in the range 0.04−2.85 mN on two iPP samples resulting in penetration depths in the range of 100−1900 nm. The ratio of residual depth and maximum depth, shown in Figure 5b, is on the order of 0.8. It is then possible that pile-up affects the measurement at larger loads although it does not for loads smaller than 130 μN. In conclusion, pile-up is not expected to cause the failure in predicting mechanical properties from nanoindentation experiments, i.e., low penetration depths.

Once shown that pile-up is not expected to play a major role on determining the analysis of the force curves, it is interesting to seek which hypothetical area function would provide the correct Young's modulus evaluation. This means that, for each sample and set of indentations at different loads, the macroscopic elastic modulus is used as an input for an indenter geometry calibration. Figure 6 shows that the apparent contact area is always larger than that obtained by calibration with fused silica and in particular for mesomorphic iPP is several times larger. The strong differences in the area functions might be explained with the pile-up, causing an increase in contact area with respect to the one calibrated on fused silica. However, deviations of this magnitude should be caused by tremendous pile-up, on the contrary of what has been shown in Figure 5, parts a and b. It is clear that pile-up cannot be responsible for the large deviations of the modulus estimated by the O&P procedure with respect to the bulk one.

A remark should be made about surface glass transition effects, because the mechanics at the near-surface might be different to the mechanics of the bulk questioning the reliability of the approach followed to obtain Figure 6. However, it is worth mentioning that this argument could affect the amorphous polymers used in this work as well as PET because their glass transition temperature is larger than room temperature. On the other side, the same is not true for iPP, with a glass transition temperature ca. 25−30 deg smaller than room temperature, a polymer that, for all the morphologies studied, shows the largest deviations in area function compared to fused silica.

Computer simulations of polymer chains in the melt showed an enrichment of chain ends on the surface on a scale of two polymer segment lengths.[28] Since there is more free volume associated with chain ends, a depletion of the surface glass temperature with respect to the bulk should thus be expected. Conclusions from previous studies on this issue are controversial since, when observed, i.e., in the case of PS,[29] the effect is restricted to a few radii of gyration, although contradictory results were reported with different techniques.[30−33]

From all these results, it is not easy to state if a lower elastic modulus should be expected at the near-surface due to a decrease of the glass transition at the surface, especially when noting that the stress field arising from a nanoindentations surely extends on a much larger volume (hundreds of nanometers) than the one interested by higher segmental mobility (fraction of or first nanometers from the surface).

Influence of Viscoelasticity. Besides pile-up, viscoelasticity is often found to be responsible for the failure of the O&P procedure

Viscoelasticity has been shown in the literature as causing a "nose" in the unloading curve;[10] i.e., the penetration depth is still increasing while the load is decreasing. A way to overcome this problem was suggested by Hochstetter et al.[3] They found that the viscoelastic effects could be minimized using a holding time, i.e., keeping the load constant at the end of the loading part, and high unloading rates. Force curves obtained with a holding time of 10 s and unloading rates of 30 μN/s for both a glassy PC and a mesomorphic iPP are drawn in Figure 7. As it can be easily seen, the "creep zone", the one where penetration depth increases at constant load during the holding time, is larger for iPP than for PC, confirming the discussion above about the higher sensitivity to viscoelastic effects for iPP. The slopes are positive immediately upon unloading, pointing out the absence of the "nose". This behavior is usually taken as a proof that viscoelastic effects are not present in principle, or at least, that the mechanical properties of the samples do not change during the time of the experiment. Such a dichotomy, implying that viscoelasticity does not contribute to the unloading exponent, i.e., that the material is not creeping to any extent, is difficult to take for grant for all the materials tested which definitely show a time dependent mechanical behavior in bulk tests.

A question arises whether the experimental conditions of this work, i.e., the choices of fast unloading and holding time before unloading, were appropriate for Young's modulus evaluation. Chudoba and Richter[34] showed indeed that the holding time had a crucial role when trying to accurately analyze force curves obtained from metals and ceramics. They also suggested values for holding time, up to 187 s in the case of aluminum.[34] In order to test this effect, we performed nanoindentations with different holding time, in the range 1−100 s finding that the differences in evaluated Young's modulus was in any case smaller than 5%, see Figure 8. This can be rationalized following Cheng and Cheng,[35] who showed that the initial unloading slope of the force curve obtained on a viscoelastic material can be divided into two terms. One of them is represented by the

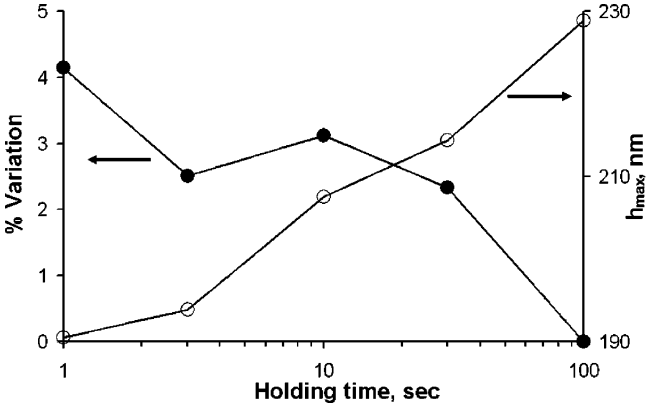

Figure 8. Changing holding time does not considerably affect Young's modulus evaluation, provided that unloading rate is fast enough. Maximum deviation is below 4%.

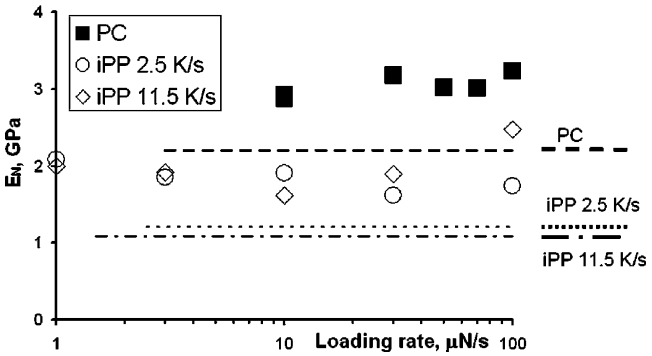

Figure 9. Dependence of elastic moduli, evaluated by Oliver and Pharr procedure, on loading rate in a broad range of conditions for three morphologies: amorphous PC and two semicrystalline iPP. Results are compared with macroscopic bulk moduli.

common relationship for purely elastic contact between S and A_c, while the other one is a function of loading history and it is negligible compared to the first term when unloading is sufficiently fast. Therefore, details of loading history are unimportant for viscoelastic materials as long as the unloading rate is sufficiently fast.[35]

Figure 9 shows a comparison of macroscopic elastic moduli and the values obtained from the unloading curve with the O&P procedure for a broad range of loading/unloading rates, from 1 to 100 μN/s, on PC and iPP solidified at two different cooling rates so that to obtain two semicrystalline samples with crystallinities and moduli decreasing with cooling rate. As expected, for the case of PC (a polymer with a very little change in Young's modulus with time/temperature in the glassy range, i.e., around room temperature) the elastic modulus is substantially unaffected by loading rate although the value drawn from nanoindentations is larger than the macroscopic one by ca. 40%. iPP is slightly more sensitive to loading rate, particularly the higher cooling rate sample, although, again, the value estimated from nanoindentations is larger than the macroscopic one by at least 100%. Another discrepancy can be found in the fact that the modulus drawn from the O&P procedure is increasingly wrong as the loading rate increases although, on decreasing test time, a smaller effect of viscoelasticity, altering the accuracy of the measurements, should be expected. As a result, it is not possible to find a loading rate condition, varied in a broad range, for which the elastic modulus, drawn from the O&P procedure, lies closer to the macroscopic one. Therefore, the results summarized by Figures 7 and 9 clearly point out that viscoelasticity should not be the source for the failure in predicting elastic modulus by the O&P procedure.

Discussion

In the O&P procedure, the unloading part of the force curve is supposed to take place in the elastic range giving thus the possibility to apply the Sneddon's theoretical analysis.[4] Sneddon indeed studied the contact between an elastic half space and a rigid punch, providing the relationship between penetration depth and applied load for different indenter geometries in the form

$$F = cp^n \tag{1}$$

where the constant c is related to mechanical properties of the sample (Young's modulus and the Poisson ratio) as well as some quantities related to indenter geometry, and the exponent n is bounded between 1 (flat-ended punch) and 2 (ideally sharp cone) depending on indenter geometry. Thus, with the knowledge of indenter shape, one should be able to estimate Young's modulus of the sample. However a problem frequently occurring is that the indenter is not a perfectly sharp cone (or pyramid) and its shape is not a priori known. To overcome this limitation, O&P suggested to differentiate eq 1 with respect to penetration depth in the case of conical punch (i.e., $n = 2$) and after some algebra one obtains the fundamental O&P equations. A final remark concerns the indenter: although a Berkovich indenter (a three sided pyramid) is commonly used for nanoindentations instead of either a flat-ended punch or a cone, it was shown that this procedure apply as well taking an equivalent semi-opening angle.[24]

On the basis of this discussion one can easily grasp the reason for the failure of the O&P procedure for which, being based on eq 1, an essential test concerns whether the Sneddon's model can properly describe contact mechanics.[16] This is a very important point because usually an O&P analysis is carried out calculating the value of contact stiffness, without checking the physical meaning of the unloading exponent[36] of eq 1. If one checks the consistency of eq 1, one observes that the experimental unloading slopes are indeed significantly larger than 2 as already anticipated in a previous work.[36] This is systematically addressed by Figure 10 for a very broad range of nanoindentations experimental conditions on the mesomorphic iPP. The disagreement between experimental results and eq 1 (not only is n is different from 2, but also it is much larger) implies that the use of the O&P analysis is improper for polymers, and the reason does not lie in the contribution of pile up or viscoelastic effects. These observations are also confirmed by a more general systematic investigation by Chaudri[15] and Lim and Chaudri,[16,37] which casts further doubts on the possibility to apply the O&P analysis in a broader range of conditions.

It was reported[35] by numerical simulations of the nanoindentation of a viscoelastic material that an increasing applied load was needed to obtain the same penetration depth, when indentation rate increased. This is in agreement with viscoelastic behavior, as the material is stiffer when tested at high loading rate. However, the contact stiffness, i.e., the slope of the unloading curve evaluated at maximum load, is independent of loading conditions in displacement controlled (DC) experiments at high enough unloading rates. Cheng and Cheng[35] clearly stated that this finding implies that the O&P procedure leads to significant errors in determining contact depth and therefore Young's modulus. We believe that the main reason for this failure is explained, from a theoretical standpoint, by Figure 10.

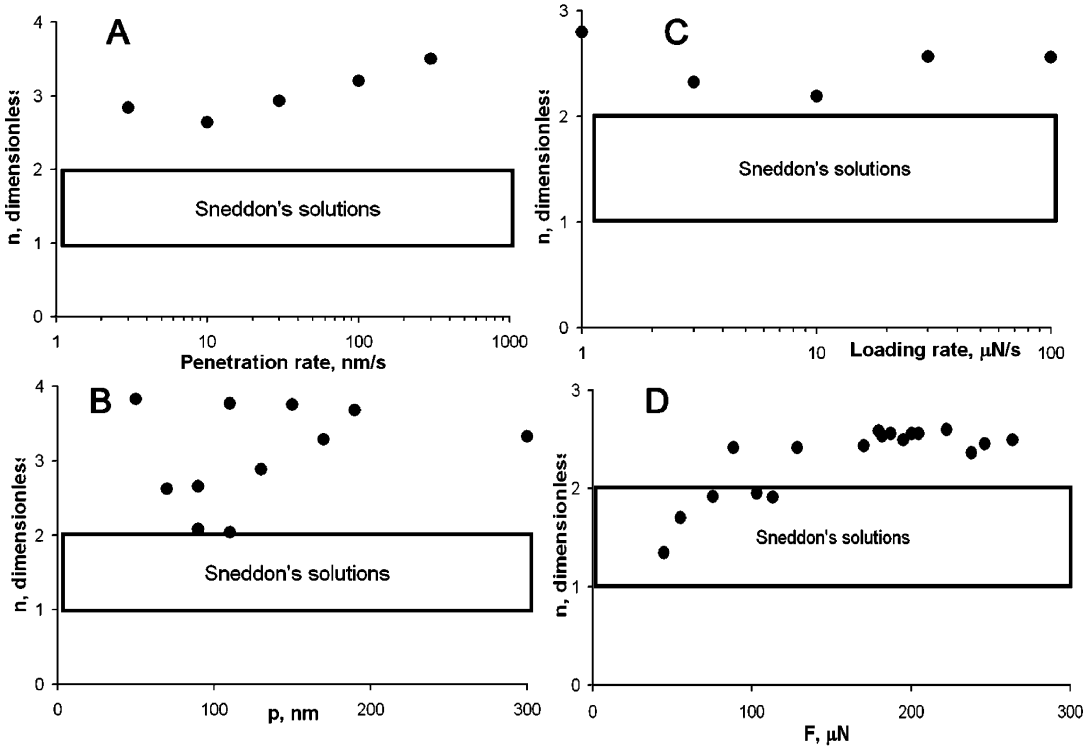

Figure 10. Unloading exponents obtained from force curves on an iPP mesomorphic sample under displacement (A, B) and load (C, D) control. Dependence on penetration rate (A) or loading rate (C) and on penetration (B) and load (D) is shown and compared to the typical range expected on the assumption[3] that an elastic contact model[4] holds.

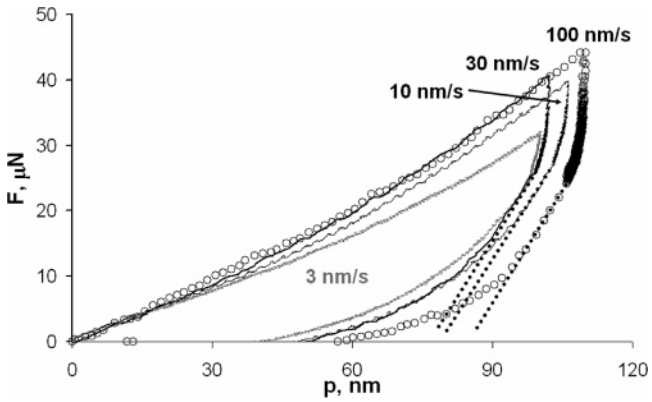

Figure 11. Unloading slopes obtained in displacement controlled mode experimentally confirms the numerical results by Cheng and Cheng.[35] As far as the unloading slopes are fast enough, the response during unloading is the same notwithstanding the loading history.

Figure 11 shows four random selected force curves, obtained in DC mode at different loading rates. Because of the difficulty to set up the feedback in DC experiments, it can be seen that the penetration depth is not kept strictly constant during the holding time. However, the maximum deviations in this latter condition in Figure 11 amounts to only 5% in the worst case, i.e., at the very fast nanoindentation of 100 nm/s. The interesting point is that these experimental results support the numerical simulations,[35] as the unloading slopes for the fast indentations (10, 30, and 100 nm/s) are evidently the same while deviations start to show up at as low indentation rate as 3 nm/s. Moreover, Figure 11 confirms the results obtained by Cheng and Cheng[35] even with the addition of a relatively short holding time.

The need for duly taking into account viscoelasticity in contact modeling however has to face the noticeable mathematical difficulty related to the complex three-dimensional stress and strain fields. Simplified models based on mechanical analogy, analytical treatments or numerical simulations have been proposed in the literature, but it is not yet clear that the fitting is sufficiently robust so that fitting parameters are representative of bulk measurable values, or moreover have physical significance. For example, a simple but rather effective approach was recently attempted by Oyen and Cook[10] based on a one-dimensional mechanical analogy of indentation with viscous-elastic-plastic elements (a spring, a linear dashpot, a quadratic dashpot for respectively elastic, viscous, and plastic response). The authors[10] succeeded to appropriately fit the force curves of two glassy, PC and PMMA, polymers, a semicrystalline polymer, PE, and a rubber, PU, polymer. Although the resultant fit did capture the nanoindentation force curve, the resulting fitting parameters may question the accuracy of the model because moduli obtained were quite unreasonable: for example, Young's moduli of 8.6, 6, and 2.8 GPa were found for, respectively, PMMA, PC, PE or a time constant of PU was found to be 12998 s.

Cheng and Cheng[35] also provided a way to measure the "modulus from the initial unloading slope". This approach seems however not to be effective: if Young's modulus for the mesomorphic iPP is evaluated from the unloading slopes of Figure 11, according to their procedure,[35] one obtains a value of 2.37 GPa, i.e., approximately 4 times the bulk one.

From these contributions and from the understanding that the stress field around the indenter tip is very complex, a proper viscoelastic contact mechanics model should instead be used to approach the analysis of force curves obtained by nanoindentations on polymers. A common feature encountered in the attempt to model the viscoelastic behavior of polymers, is the use of a constant viscoelastic Poisson ratio, PR in the following. PR is actually not only time dependent, but also load history dependent even within the framework of linear viscoelasticity, because it is by its very nature a nonlinear function of pair of perpendicular strains[38−40] (including cases when materials obey linear constitutive relations). A constant value of the viscoelastic

PR is physically coherent only for incompressible materials when PR is equal to 0.5.[38−40] This led Hilton[38−40] to state that "under all other circumstances constant PR values represent extremely restrictive conditions for real materials". For example, alternatively to incompressible materials, another possible condition for time independent PR is a value approaching 0.5 and $K \gg G$; on the other hand, for most materials, K, the bulk modulus, is only larger than G, the shear modulus. This example clearly shows how restrictive the assumption of a constant PR is.

All these arguments seem to indicate that the evaluation of Young's modulus of polymers by nanoindentations is not yet accessible. However, it is worth mentioning that this task has been accomplished recently through the use of a phenomenological correction factor of the O&P procedure[41] as well as by atomic force microscopy nanoindentations.[42−44] Taking advantage of the very small scale and the peculiar shape of the indenter, which introduce favorable conditions for the onset of a size scale effect,[44] it was possible to carry out nanoindentations such that residual indentation depth is 1 order of magnitude smaller than penetration under full load,[44] thus the material response is mainly elastic. This allows one to apply elastic contact mechanics models, without violating any theoretical assumption and accessing the mechanical properties of single nanophases.[45]

Conclusions

The Oliver and Pharr procedure cannot estimate Young's modulus of polymers through nanoindentations. This failure is commonly attributed to pile-up or viscoelastic effects. It is shown in this work that although pile-up contributions can be minimized at shallow enough penetration depths, still Young's modulus evaluated by the O&P procedure gives rise to significant deviations with respect to the value measured macroscopically. On the other hand viscoelasticity, often identified in a "nose" in the force curve,[10] could be minimized performing indentations at large loading rates.[3] Again the elastic modulus drawn from the O&P procedure by nanoindentations in a very broad range of loading rates is consistently higher that the bulk Young's modulus.

The reason for this failure has to be found in the peculiar mechanical behavior of polymers: viscoelasticity changes the nanoindentation contact mechanics with respect to the elastic one, and the unloading exponent is always larger than 2 even at very high indentation rates. A quadratic relation can be considered as a bound for elastic behavior, as suggested by Sneddon,[4] and an exponent larger than 2 means that the Oliver and Pharr procedure, as well as any other procedure derived from elastic contact mechanics, cannot be applied to the unloading curve even though the typical "viscoelastic nose" is not found in the force curve.

A phenomenological correction factor has been recently introduced in order to correctly evaluate Young's modulus of polymers by nanoindentations.[41] Alternative to this approach, AFM nanoindentations represent a useful tool for this task.[42−44]

Acknowledgment. The authors acknowledge the financial support of the Ph.D. grant of D.T. by the University of Palermo and the financial support from the Italian Ministry of University and Scientific Research (MIUR, Italy), PRIN04 grant. We also acknowledge the support of the European Science Foundation through a Short-Term Scientific Mission in the framework of COST P12, Structuring of Polymers, Action. Finally D.T. is particularly grateful to Drs. B. Beake and K. Narain of MicroMaterials, Wrexham, U.K., for help and support on the experiments carried out with the Nanotest 600 nanoindenter.

Appendix

Let us examine a sample with rectangular cross section under an external compression load. This portion of calculations, which follow, is limited to the elastic range only. The scheme of forces acting is presented in the sketch, where the force acts only along y direction while both surfaces perpendicular to the x and z directions are confined.

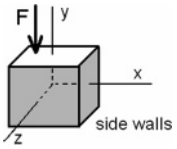

The elasticity equations for an isotropic body may be written as

$$\epsilon_y = \frac{1}{E}(\sigma_y - \nu\sigma_x - \nu\sigma_z)$$

$$\epsilon_x = \frac{1}{E}(\sigma_x - \nu\sigma_y - \nu\sigma_z) = 0$$

$$\epsilon_z = \frac{1}{E}(\sigma_z - \nu\sigma_y - \nu\sigma_x) = 0$$

Assuming, for symmetry considerations, that the stress in x and z directions is the same, $\sigma_x = \sigma_z$, it follows that

$$\epsilon_y = \frac{1}{E}\left(1 - \frac{2\nu^2}{1-\nu}\right)\sigma_y$$

Therefore Young's modulus in full confinement geometry is

$$\sigma_y/\epsilon_y = \frac{E}{(1-2\nu^2)/(1-\nu)}$$

This implies that, for an incompressible material, Young's modulus diverges. For a material with Poisson ratio equal to approximately 0.3, i.e., several polymers, Young's modulus under full confinement is 35% larger than the one under uniaxial compression.

References and Notes

(1) Yang, S.; Zhang, Y.-W.; Zeng, K. *J. Appl. Phys.* **2004**, *95*, 3655.
(2) Oliver, W. C.; Pharr, G. M. *J. Mater. Res.* **1992**, *7*, 1564.
(3) Hochstetter, G.; Jimenez, A.; Loubet, J. L. *J. Macromol. Sci., B: Phys.* **1999**, *38*, 681.
(4) Sneddon, I. N. *Int. J. Eng. Sci.* **1965**, *3*, 47.
(5) Hay, J. C.; Bolshakov, A.; Pharr, G. M. *J. Mater. Res.* **1999**, *14*, 2296.
(6) King, R. B. *Int. J. Solids Struct.* **1987**, *23*, 1657.
(7) Bolshakov, A.; Pharr, G. M. *J. Mater. Res.* **1998**, *13*, 1049.
(8) Field, J. S.; Swain, M. V. *J. Mater. Res.* **1993**, *8*, 297.
(9) Loubet, J. L.; Georges, J. M.; Meille, J. *Nanoindentation Techniques in Materials Science and Engineering*; ASTM: Philadelphia, PA, 1986.
(10) Oyen, M. L.; Cook, R. F. *J. Mater. Res.* **2003**, *18*, 139.
(11) Ting, T. C. T. *J. Appl. Mech.* **1966**, *33*, 845.
(12) Hengsberger, S.; Kulik, A.; Zysset, P. *Bone* **2002**, *30*, 178.
(13) Troyon, M.; Huang, L. *J. Mater. Res.* **2005**, *20*, 610.
(14) Ikezawa, K.; Maruyama, T. *J. Appl. Phys.* **2002**, *91*, 9689.
(15) Chaudri, M. M. *J. Mater. Res.* **1999**, *16*, 33.
(16) Lim, Y. Y.; Chaudri, M. M. *Philos. Mag.* **2003**, *83*, 3427.
(17) Tranchida, D.; Piccarolo, S. *Polymer* **2005**, *46*, 4032.
(18) Ward, I. M.; *Mechanical properties of solid polymers*; John Wiley & Sons: Chichester, U.K., 1983.
(19) Piccarolo, S.; Saiu, M.; Brucato, V; Titomanlio, G. *J. Appl. Polym. Sci.* **1992**, *46*, 625.
(20) Piccarolo, S. *J. Macromol. Sci., Phys. B.* **1992**, *31*, 501.

(21) La Carruba, V.; Brucato, V; Piccarolo, S. *J. Polym. Sci., B: Polym. Phys.* **2002**, *1*, 153.
(22) Brucato, V.; Piccarolo, S.; La Carrubba, V. *Chem. Eng. Sci.* **2002**, *57*, 4129.
(23) Piccarolo, S. *Polymer* **2006**, *47*, 5610.
(24) Oliver, W. C.; Pharr, G. M. *J. Mater. Res.* **2004**, *19*, 3.
(25) Pharr, G. M.; Bolshakov, A. *J. Mater. Res.* **2002**, *17*, 2660.
(26) Martin, M.; Troyon, M. *J. Mater. Res.* **2002**, *17*, 2227.
(27) Mott, B. W.; *Micro-indentation hardness testing*; Butterworths: London, 1956.
(28) Wu, X. Z.; Ocko, B. M.; Sirota, E. B.; Sinha, S. K.; Deutsch, M.; Cao, B. H.; Kim, M. W. *Science* **1993**, *261*, 1018.
(29) Liu, Y.; Russell, T. P.; Samant, M. G.; Stohr, J.; Brown, H. R.; Cossy-Favre, A.; Diaz, J. *Macromolecules* **1997**, *30*, 7768.
(30) Xie, L.; DeMaggio, G. B.; Frieze, W. E.; DeVries, J.; Gidley, D. W.; Hristov, H. A.; Yee, A. F. *Phys. Rev. Lett.* **1996**, *74*, 4947.
(31) Tsui, O. K. C.; Wang, X. P.; Ho, J. Y. L.; Ng, T. K.; Xiao, X. *Macromolecules* **2000**, *33*, 4198.
(32) Kaijiama, T.; Tanaka, K.; Takahara, A. *Macromolecules* **1995**, *28*, 3482.
(33) Hammerschmidt, J. A.; Gladfelter, W. L.; Haugstad, G. *Macromolecules* **1999**, *32*, 3360.
(34) Chudoba, T.; Richter, F. *Surf. Coat. Technol.* **2001**, *148*, 191.
(35) Cheng, Y. T.; Cheng, C. M. *J. Mater. Res.* **2005**, *20*, 1046.
(36) Tranchida, D.; Piccarolo, S. *Macromol. Rap. Comm.* **2005**, *26*, 1800.
(37) Lim, Y. Y.; Chaudhri, M. M. *J. Appl. Phys.* **2005**, *98*, 73518.
(38) Hilton, H. H.; Yi, S. *Int. J. Solids Struct.* **1998**, *35*, 3081.
(39) Hilton, H. H.; *An introduction to viscoelastic analysis in: Engineering design for plastics*; E. Boer Reinhold Publishing Corp.: New York, 1964.
(40) Hilton, H. H. *Mech. Comp. Mat. Str.* **1996**, *3*, 97.
(41) Tranchida, D.; Piccarolo, S.; Loos, J.; Alexeev, A. *Appl. Phys. Lett.* **2006**, *89*, 171905.
(42) Tsukruk, V. V.; Huang, Z.; Chizhik, S. A.; Gorbunov, V. V. *J. Mater. Sci.* **1998**, *33*, 4905.
(43) Cappella, B.; Kaliappan, S. K.; Sturm, H. *Macromolecules* **2005**, *38*, 1874.
(44) Tranchida, D.; Piccarolo, S.; Soliman, M. *Macromolecules* **2006**, *39*, 4547.
(45) Tranchida, D.; Kiflie, Z.; Piccarolo, S. *Macromol. Rapid Commun.* **2006**, *27*, 1584.

MA062140K